Delineation of molecular mechanisms of sensitivity to lapatinib in breast cancer cell lines using global gene expression profiles

Priti S. Hegde,[1] David Rusnak,[2] Melissa Bertiaux,[1] Krystal Alligood,[2] Jay Strum,[1] Robert Gagnon,[3] and Tona M. Gilmer[2]

Departments of [1]Genomic and Proteomic Sciences, [2]Translational Medicine, and [3]Computational, Analytical, and Structural Sciences, GlaxoSmithKline, Inc., Research Triangle Park, North Carolina

Abstract

Lapatinib (GW572016) is a small-molecule dual inhibitor of epidermal growth factor receptor (ErbB1) and ErbB2 receptor kinase activities currently in phase III clinical trials. We used phosphoprotein and microarray analyses to carry out targeted pathway studies of phosphorylation and gene expression changes in human breast cancer cell lines in the presence or absence of lapatinib. Studies were done in four breast cancer cell lines, two of which were responsive and two of which were nonresponsive to lapatinib. Responsive cell lines, BT474 and SKBr3, constitutively overexpress ErbB2 and show an IC_{50} of 25 or 32 nmol/L for lapatinib, respectively. In contrast, nonresponsive MDA-MB-468 and T47D cells expressed a low basal level of ErbB2 and showed IC_{50} values in the micromolar range. Cells responsive to lapatinib exhibited strong differential effects on multiple genes in the AKT pathway. After 12 h of exposure to 1.0 μmol/L of lapatinib, *AKT1*, *MAPK9*, *HSPCA*, *IRAK1*, and *CCND1* transcripts were down-regulated 7- to 25-fold in responsive BT474 and SKBr3 cells. In contrast, lapatinib weakly down-regulated the AKT pathway in nonresponsive breast cancer cell lines (<5-fold down-regulation of most genes in the pathway). Furthermore, the proapoptotic gene *FOXO3A*, which is negatively regulated by AKT, was up-regulated 7- and 25-fold in lapatinib-responsive SKBr3 and BT474 cells, respectively. Phosphorylated Akt and Akt-mediated phosphorylation of FOXO3A also decreased in responsive breast cancer cell lines exposed to lapatinib. Gene expression profiling also revealed that lapatinib stimulated the expression of estrogen and progesterone receptors and modulated the expression of genes involved in cell cycle control, glycolysis, and fatty acid metabolism. In BT474 and T47D cells, which expressed moderate basal levels of the estrogen and progesterone receptors, 1.0 μmol/L of lapatinib induced expression by 7- to 11-fold. These data provide insight into the mechanism of action of lapatinib in breast cancer cells. [Mol Cancer Ther 2007;6(5):1629–40]

Introduction

The ErbB receptor tyrosine kinase family includes multidomain proteins with an extracellular ligand binding domain, a single transmembrane domain, and an intracellular tyrosine kinase domain. The family has three catalytically active members, epidermal growth factor receptor (EGFR; ErbB1), ErbB2, and ErbB4, and one catalytically inactive member, ErbB3 (1, 2). These proteins form heterodimeric and homodimeric membrane receptor complexes that mediate the proliferative effects of several common growth factors including epidermal growth factor, transforming growth factor-α, and heregulin (3, 4). Dimerization and phosphorylation of tyrosine residues on the cytoplasmic tail of ErbB receptors create specific binding sites for adapter proteins such as src-homology 2 domain–containing proteins. The recruitment of proteins to the receptor activates signal transduction pathways, e.g., mitogen-activated protein kinase/extracellular signal-regulated kinase, signal transducers and activators of transcription, and phosphatidylinositol-3-kinase/Akt (5). As a result of the signaling cascade, EGFR and ErbB2 play critical roles in ligand-activated signaling pathways that regulate cell proliferation and cell death. Many tumors overexpress these receptors and/or display constitutive activation of these pathways; therefore, these proteins are considered likely targets for antitumor drugs.

Several small molecules specifically targeted to EGFR and/or ErbB2 receptor tyrosine kinases are currently approved or are in late stage clinical trials, including gefitinib (ZD-1839 Iressa), erlotinib (OSI-774, Tarceva), lapatinib (GW572016 Tykerb), and HKI-272 (6–8). Lapatinib is a reversible dual inhibitor of EGFR and ErbB2, currently in phase III clinical trials for breast cancer (9–11), whereas HKI-272 is an irreversible dual inhibitor in phase II clinical trials for breast and lung cancer (8). Gefitinib and erlotinib are selective EGFR inhibitors approved for the treatment of lung cancer (12).

The role of growth factor and steroid hormone receptors in human breast cancer has been given considerable attention. Overexpression of the EGFR and ErbB2 receptor

Received 10/3/05; revised 2/21/07; accepted 3/30/07.

The costs of publication of this article were defrayed in part by the payment of page charges. This article must therefore be hereby marked *advertisement* in accordance with 18 U.S.C. Section 1734 solely to indicate this fact.

Note: Current address for P.S. Hegde: Department of Development Sciences, Genentech Inc., 1 DNA Way, South San Francisco, CA 94080.

Requests for reprints: Tona M. Gilmer, Department of Translational Medicine, GlaxoSmithKline, Inc., 5 Moore Drive, Research Triangle Park, NC 27709. Phone: 919-483-2100; Fax: 919-315-3749. E-mail: tona.m.gilmer@gsk.com

doi:10.1158/1535-7163.MCT-05-0399

tyrosine kinases is associated with poor survival in patients with breast cancer (13, 14), as is loss of expression of estrogen receptor (ER) and/or progesterone receptor (PR; ref. 15). Some studies suggest that the expressions of ER and PR are inversely correlated with the expressions of EGFR and ErbB2 in breast cancer (16, 17). However, ~11% to 19% of ER-positive tumors also express ErbB1, ErbB2, or ErbB3 at a high level (15, 18). Ten-year survival was lower for patients with tumors positive for both ER and ErbB1/ErbB2/ErbB3 (35%) than for those with ER+ tumors negative for all ErbB receptors (55%; ref. 15).

Several studies have reported the importance of the cross-talk between ErbB1 and ErbB2 and ER networks in breast cancer growth and development, and as a mechanism for endocrine resistance (19–21). These results, as well as additional studies, suggest that combination therapy targeting the estrogen and/or PRs and EGFR and ErbB2 could be useful (22–24). Preclinical data indicate that lapatinib cooperates with tamoxifen to inhibit cell proliferation and signaling in antiestrogen-resistant breast cancer cell lines (25). In addition, a phase I clinical trial combining lapatinib and letrozole in ER/PR+ advanced breast cancer and other tumors, such as ovarian and endometrial tumors, have shown encouraging results (26). Phase III trials with this combination are ongoing.

This report examines the effects of dual EGFR/ErbB2 inhibitor lapatinib on gene expression in four human breast cancer cells, two of which are responsive to lapatinib and two of which are nonresponsive. Phosphoprotein analysis confirmed that phosphorylation and activation of AKT decreases in response to lapatinib. Gene expression profiling was carried out on these four cell lines using the U133A Affymetrix human 22,000-element microarray. cDNA was prepared from cells grown in the presence or absence of high- or low-dose lapatinib and hybridized to the array. Bioinformatic analysis identified genes and pathways differentially expressed in lapatinib-responsive cell lines. The results show strong down-regulation of the AKT pathway in responsive but not in nonresponsive cell lines. Furthermore, the proapoptotic FOXO3A subpathway, which is negatively regulated by AKT, is differentially upregulated in drug-treated responsive cells. Lapatinib induced transcription of *ESR1* and *PGR*, the genes for ER and PR in two of the four breast cancer cell lines, emphasizing the importance of the cross-talk between the Erb receptors and the steroid hormone pathways. Lapatinib also has differential effects on genes involved in cell cycle control, glycolysis, and fatty acid metabolism.

Materials and Methods

Cells and Cell Culture

MDA-MB-468 (MDA468), SK-Br-3 (SKBr3), T-47D (T47D), and BT-474 (BT474) breast tumor cell lines were obtained from the American Type Culture Collection. The LICR-LON-HN5 (HN5) head and neck carcinoma cell line was a gift from Helmout Modjtahedi at the Institute of Cancer Research, Surrey, United Kingdom. They were used as a control for EGFR RNA and protein levels because they overexpress EGFR. HN5 cells were grown in low glucose DMEM (Invitrogen) containing 10% fetal bovine serum. MDA468 cells were cultured in DMEM (Invitrogen) containing 10% fetal bovine serum (HyClone). SKBr3, T47D, and BT474 were cultured in RPMI 1640 (RPMI; Invitrogen) containing 10% fetal bovine serum. Cells were plated in 100 mm tissue culture dishes (Becton Dickinson) and allowed to grow until cells were ~70% confluent. All cells were cultured in a humidified incubator at 37°C in 95% air/5% CO_2.

Compound Treatment

Powdered lapatinib (GW572016F) was synthesized as previously described (27) and dissolved in neat DMSO (Sigma-Aldrich Chemical Company) at 10 mmol/L. The 10 mmol/L stock was serially diluted in neat DMSO to make stocks of 1 and 0.1 mmol/L. The serially diluted DMSO stocks of lapatinib were added to the appropriate growth medium for each cell line at a 1:1,000 dilution to make treatment solutions of 1 and 0.1 μmol/L in growth media. These solutions contained 0.1% DMSO; a vehicle control containing 0.1% DMSO was also made. The media from the cell plates were aspirated and 10 mL of medium containing vehicle, 1, or 0.1 μmol/L of lapatinib were added to each of triplicate plates. Cells were returned to the incubator and treated for the times described in the data tables. After appropriate incubation times, the media were aspirated and 3 mL of TRIzol Reagent (Invitrogen) were added to each plate. The plates were scraped to ensure the removal of all cells. The lysate was collected into 15 mL polypropylene tubes and transferred to a −80°C freezer.

Cell Culture IC_{50} Determination. For IC_{50} determination, cells were plated in the appropriate medium at plating densities that resulted in logarithmic growth for the duration of the assay and returned to the incubator overnight. Twenty-four hours after initial seeding, cells were exposed to lapatinib. Cells were dosed in 50% native medium and 50% low glucose DMEM containing 5% fetal bovine serum, 50 μg/mL gentamicin, and 0.3% DMSO with 10 GW572016F concentrations ranging from 30 to 0.00152 μmol/L. After 72 h of compound exposure, media were removed by aspiration. Cell biomass was estimated by staining cells in 0.1 mL per well of methylene blue (0.5% in 50:50, ethanol/water; Sigma), followed by incubation at room temperature for at least 30 min. Stains were aspirated and the plates rinsed by immersion in deionized water followed by air-drying. Stains were released from cells by the addition of 0.1 mL of solubilization solution (1.0% *N*-lauroyl sarcosine, sodium salt in PBS; Sigma). Plates were incubated at room temperature for 40 min. Plates were read at 620 nmol/L in a microplate reader. Percent inhibition of cell growth was calculated relative to untreated control wells. Percent inhibition of cell growth was calculated relative to untreated control wells. Growth inhibition data were fitted to the four-parameter Hill model, $y = E_{max} \times (1 - [x^n / (K^n + x^n)]) + E_{min}$, using the method of Levenberg and Marquardt (summarized in

ref. 28), with E_{max} estimated based on 100% growth of vehicle treated cells, E_{min} defined as background signal (no cells) and K equal to the IC_{50}.

Protein Lysate Preparation. Cells plated in 100 mm dishes were treated with lapatinib or vehicle at specified doses for specified time points, as described above. Cells were rinsed with cold PBS and lysed in 300 μL of radioimmunoprecipitation assay buffer plus [150 mmol/L NaCl, 50 mmol/L Tris-HCl (pH 7.5), 0.25% deoxycholate, 1% NP40, 1 mmol/L sodium orthovanadate (Sigma), Calbiochem phosphatase inhibitor cocktail, and protease inhibitor cocktail (Roche)] per 100 mm dish. Cells were scraped and transferred to microfuge tubes for sonication, and lysates were clarified by centrifugation.

Antibodies. The Western blotting antibody cocktail for EGFR (anti-EGFR Ab-12, R19/48), the immunoprecipitating antibody cocktail for EGFR (anti-EGFR Ab-13, clone 528 + 199.12), the dissociation-enhanced lanthanide fluorescent immunoassay (DELFIA) detection antibody for EGFR (anti-EGFR Ab-17), and the DELFIA capture antibody for ErbB2 (anti–c-ErbB2/Her-2/*neu* Ab-4, clone N12) were purchased from Lab Vision. ErbB2 immunoprecipitating and Western blotting antibody, anti–c-*neu* Ab-3, was purchased from Oncogene Research Products. Antiphosphotyrosine monoclonal antibody, PT-66, was purchased from Sigma. Anti–phospho-Akt (Ser^{473}) Ab 9271 and monoclonal anti–cyclin D1 (clone DCS6) were purchased from Cell Signaling Technology. Anti–phospho-FKHRL1 (Thr^{32}) antibody (06-952) and the EGFR DELFIA capture antibody, anti-EGFR clone LA1 (05-101), were purchased from Upstate Biotechnology, Inc. The DELFIA ErbB2 detection antibody, anti-Neu (C-18), and the anti-Akt polyclonal antibody (sc-8312) were purchased from Santa Cruz Biotechnology, Inc. The Western blotting antibody for p27 (clone 57) was purchased from BD Transduction Laboratories. Europium-conjugated goat anti-rabbit IgG (AD0105) was purchased from Perkin-Elmer. Horseradish peroxidase–conjugated donkey anti-mouse and anti-rabbit secondary antibodies were purchased from Jackson Immunoresearch Laboratories, Inc. IRDye800-conjugated goat anti-rabbit IgG secondary antibody for Odyssey Infrared Imaging analysis was purchased from Rockland, Inc., and Alexa-Fluor 680–conjugated goat anti-mouse IgG secondary antibody for imaging analysis was purchased from Molecular Probes.

Western Blot Analysis. Lysates were prepared for SDS-PAGE at 1 mg/mL in 1× Novex Tris-Glycine SDS sample buffer (Invitrogen) containing 2.5% β-mercaptoethanol. Twenty micrograms of each sample were resolved on Novex Tris-Glycine gels (Invitrogen) and were transferred to nitrocellulose (Invitrogen). Membranes were blocked in TBST [150 mmol/L NaCl, 10 mmol/L Tris-HCl (pH 7.5), and 0.1% Tween 20] containing 4% (w/v) bovine serum albumin or milk for Western blot analysis using enhanced chemiluminescence (ECL, Amersham) for detection. For Western blot analysis using the Odyssey Infrared Imaging System, membranes were blocked in Odyssey Blocking Buffer (Licor). Membranes were blotted for Akt and phospho-Akt resolved on 8% gels with antibodies diluted 1:2,000 and 1:1,000, respectively, in TBST containing 4% bovine serum albumin and 2% milk. Horseradish peroxidase–conjugated donkey anti-rabbit secondary antibody was diluted 1:5,000 in blocking buffer, and ECL (Amersham) was used for detection. Phospho-FKHRL1 (Thr^{32}) in BT474, MDA-468, and T47D cells was blotted with the polyclonal antibody diluted 1:1,000 in TBST containing 4% bovine serum albumin. Horseradish peroxidase–conjugated donkey anti-rabbit IgG was diluted 1:10,000 and ECL was used for detection. For detection of phospho-FKHRL1 in SKBr3 cells, the membrane was blocked in Odyssey Blocking Buffer and the antibody was diluted 1:1,000 in Odyssey Blocking Buffer containing 0.1% Tween 20. The membrane was washed with PBS (Invitrogen) without calcium and magnesium salts and containing 0.1% Tween 20. The secondary antibody, IRDye800 goat anti-rabbit IgG, was diluted 1:1,000 in Odyssey Blocking Buffer containing 0.1% Tween 20. IR imaging was used for visualization. The membrane for detection of p27 on a 10% to 20% gel was blocked in TBST containing 4% milk. Anti-p27 monoclonal antibody was diluted 1:1,000 in the same blocking buffer. Horseradish peroxidase–conjugated donkey anti-mouse secondary antibody was diluted 1:2,500 and ECL was used for detection.

Detection of ErbB Receptor Levels by Western Blot. Lysates were prepared for SDS-PAGE at 1 mg/mL in 1× Novex Tris-Glycine SDS sample buffer (Invitrogen) containing 2.5% β-mercaptoethanol, and 20 μg of the lysate was loaded on duplicate 6% Novex Tris-Glycine gels (Invitrogen). For cell lines known to overexpress EGFR or ErbB2, lysates were diluted to 0.1 mg/mL and 2 μg was loaded on the appropriate gel for the overexpressed receptor. Lysates were resolved by electrophoresis and transferred to nitrocellulose membranes. The membranes were blocked overnight at 4°C in TBST containing 4% bovine serum albumin. Membranes were immunoblotted for EGFR or ErbB2 with antibodies diluted 1:1,000 in blocking buffer. Horseradish peroxidase–conjugated AffiniPure Donkey Anti-Mouse IgG (H+L) was diluted 1:10,000 in blocking buffer and ECL was used for detection. The intensities of bands corresponding to EGFR and ErbB2 were quantified by densitometry using the Bio-Rad Fluor S Multi-imager. The amount of receptor per microgram of lysate was calculated for each cell line and was expressed as a percentage of EGFR in HN5 cells which overexpress EGFR, or ErbB2 in BT474 cells which overexpress ErbB2.

For Western blot analysis of phosphorylated receptors, receptors were immunoprecipitated from cell lysates using the appropriate antibodies. Immunoprecipitated receptors were resolved on 6% Novex gels (Invitrogen) and transferred to nitrocellulose membranes. Membranes were probed with antiphosphotyrosine monoclonal antibody PT-66 diluted 1:1,000. ECL was used for detection.

Detection of ErbB Receptor Levels by DELFIA. Monoclonal antibodies for capturing EGFR or ErbB2 were diluted to 3 μg/mL in PBS containing calcium chloride and magnesium chloride (Sigma). Wells of PolySorp 96-well

assay plates (Nunc) were coated overnight at 4°C with 100 μL of antibody per well. Wells were rinsed four times with deionized water and blocked with 300 μL of TBST containing 4% bovine serum albumin for at least 2 h at room temperature. Cell lysates were diluted in 2 mL deep-well plates to 20 μg/mL in radioimmunoprecipitation assay buffer plus, and serially diluted to 10 and 5 μg/mL. Wells of the assay plates were rinsed four times with distilled water and 100 μL of the lysates were transferred to appropriate wells. Plates were kept at 4°C overnight. Wells were washed four times with TBST, followed by incubation with 100 μL of EGFR or ErbB2 polyclonal detection antibodies diluted 1:2,500 in blocking buffer. After incubating for 1 h at room temperature, wells were washed again as before and 100 μL of Europium-conjugated goat anti-rabbit IgG, diluted 1:10,000 in blocking buffer, were added. Following incubation for 1 h at room temperature, wells were washed four times with TBST and 100 μL of DELFIA enhancement solution (Perkin-Elmer) were added. After 10 min, Europium fluorescence was measured using a Victor Multilabel Counter (Wallac). Background wells were averaged and the average background was subtracted from all wells. Duplicate wells were averaged for all of the lysate samples. Linearity of the signal for the highest expressers EGFR and ErbB2 over the concentration range tested was confirmed. Measurements for all cell lines at the highest concentrations within the linear range were averaged and expressed as a percentage of the average measurement for HN5 lysate or BT474 lysate (for EGFR or ErbB2, respectively).

RNA Sample Preparation and Processing

Cells plated in triplicate were lysed in TRIzol, the cell lysate was extracted with chloroform, and RNA was purified from the lysate using the QIAGEN RNeasy Mini Kit (QIAgen, Inc.). cDNA was prepared from 5 μg of total RNA using the Invitrogen SuperScript Double-Stranded cDNA Synthesis Kit (Invitrogen, Inc.). cDNA was amplified and biotinylated using the ENZO BioArray High-Yield RNA Transcript Labeling Kit (Enzo Biochem, Inc.). The amplified cDNA samples were fragmented and hybridized onto HG-U133A GeneChips. After sample hybridization, arrays were washed, stained, and scanned according to the standard Affymetrix protocol.

Data Analyses

Gene expression data were analyzed using Microarray Analysis Suite 5.0 software (Affymetrix). Signal intensities were obtained by scaling all hybridized chips to a target intensity of 150. Raw data files (.CEL) were exported into the Rosetta Resolver database (version 3.2, Rosetta Biosoftware). The data has also been deposited in ArrayExpress with accession no. E-MEXP-440.[4] Three independent replicates were used for each treatment condition. Error-adjusted fold change (xdev) was calculated for each gene sequence on the gene chip using the Resolver error model (29). To identify gene signatures associated with responsive cells, the xdev values for each condition were exported into Spotfire DecisionSite (version 7.1.1, Spotfire). The Pearson's correlation metric within DecisionSite was used to select genes with similar expression profiles across the four cell lines. Pathways of relevance were identified using a proprietary pathway analysis tool (Zoompath) which uses protein-protein and protein-DNA associations from a variety of proprietary and public databases to identify and analyze gene interaction networks (30).

Results

Previous studies tested the efficacy and selectivity of lapatinib in inhibiting the growth of human tumor and nontumor cells. These studies showed that lapatinib resulted in potent growth inhibition of human HN5 (head and neck), A-431 (epidermal), BT474 (breast), CaLu-3 (lung), and N87 (gastric) tumor cells (9). In contrast, the IC_{50} values were ~20-fold higher for control cells including human foreskin fibroblasts, nontumorigenic epithelial cells, and nonoverexpressing breast cancer cells (MCF-7 and T47D). The previous study identified MCF-7 and T47D as breast cancer cell lines that did not respond well to the antiproliferative effects of lapatinib and correlated their nonresponsiveness to the low levels of EGFR and ErbB2 expression in those cell lines. Here, the determinants of responsiveness to lapatinib in human breast cancer cells were analyzed more closely using targeted gene expression profiling of two responsive breast tumor cell lines, BT474 and SKBr3, and the nonresponsive breast cancer cell lines, T47D and MDA468.

Table 1 summarizes initial characterization of drug responsiveness in BT474, SKBr3, T47D, and MDA468 cancer cell lines. BT474 and SKBr3 cells have IC_{50} values for growth inhibition of 25 and 32 nmol/L, respectively, whereas MDA468 and T47D cells have ≈100-fold higher IC_{50} values of 2.3 and 4.8 μmol/L, respectively. Previous studies show that lapatinib binds with high affinity to EGFR and ErbB2 (10) and is a potent inhibitor of the tyrosine kinase activity of both of these receptors (9, 10). Previous studies also suggest that susceptibility to lapatinib correlates with high overexpression of EGFR or ErbB2 (9, 31). EGFR RNA and protein levels were compared with HN5 cells which overexpress EGFR, whereas ErbB2 RNA and protein levels were compared with BT474 cells which overexpress ErbB2. Table 1 shows that basal expression of ErbB2 protein is high in BT474 and SKBr3 cells, but is low in MDA468 and T47D cells. In contrast, basal expression of EGFR protein is low in three of the breast cancer cell lines. Only MDA468 cells express a high basal level of EGFR. These results suggest that overexpression of EGFR in human breast cancer cells may not be sufficient to confer responsiveness to lapatinib, or that MDA468 cells may be deficient in one or more downstream factors required for lapatinib-induced blocking of EGFR signaling. Basal transcription of *EGFR* and *ERBB2* was also determined using microarray analysis on the 22,000-element human Affymetrix U133A array, which

[4] http://www.ebi.ac.uk/arrayexpress/

Table 1. Antiproliferative activity of lapatinib and RNA and protein levels in breast cancer cell lines

	IC_{50}*	ErbB2† RNA	ErbB2‡ Western	ErbB2‡ DELFIA	EGFR† RNA	EGFR‡ Western	EGFR‡ DELFIA
BT474	0.025 ± 0.004	100.0	100.0	100.0	2.2	0.4	0.5
SKBR3	0.032 ± 0.005	91.0	103.0	66.0	4.9	0.34	0.68
T47D	4.83 ± 1.12	3.8	1.2	2.3	1.4	0.03	0.53
MDA468	2.32 ± 0.21	1.5	0.1	Below the limit of detection	5.6	66.0	50.0

*IC_{50} (μmol/L) for the indicated cell lines in the presence of lapatinib. Error is SE.
†ErbB-2 and EGFR RNA were quantified as described in Materials and Methods.
‡ErbB-2 and EGFR protein were quantified as described in Materials and Methods.

quantifies expression of 14,500 well-characterized human genes. The results show that the relative levels of EGFR and ErbB2 mRNA correspond closely to the levels of EGFR and ErbB2 protein in these cells (Table 1). The normalized intensity of ErbB2 transcripts was 6,000 to 7,000 in the responsive cell lines but less than 500 in the nonresponsive cell lines. It should be pointed out that ≈95% of all transcripts on the microarray chip had normalized intensities in the range of 0 to 500. Thus, ErbB2 mRNA is very highly overexpressed in BT474 and SKBr3 cells. Both EGFR and ErbB2 proteins were phosphorylated in BT474, SKBR3, and T47D cells, whereas pEGFR could only be detected in MDA468 due to the very low levels of ErbB2 protein. Lapatinib decreases pEGFR and pErbB2 in these cell lines in a dose-dependent manner (Fig. 1A). The inhibition of pEGFR in MDA468 is ~4-fold lower than in BT474, for example, and may contribute to the higher IC_{50} for response.

The effects of lapatinib on gene expression in responsive and nonresponsive human breast cancer cells were analyzed in detail. Microarray analysis with the Affymetrix U133A chip was used to identify pathways in which multiple genes were strongly differentially expressed in responsive cells. This analysis indicated strong differential effects on the AKT pathway in response to lapatinib, which is consistent with previous studies showing lapatinib-mediated suppression of AKT-phosphorylation in responsive cells (9, 32). Microarray and phosphoprotein studies describing the effects of lapatinib on several genes in the AKT pathway are summarized in Figs. 1 and 2 and Table 2.

As shown in Fig. 1B, AKT phosphorylation on Ser^{473} decreases significantly in BT474 and SKBr3 cells exposed to lapatinib for 6 h, but only slightly in the nonresponsive cells. Total AKT protein levels remained unchanged during this 6-h period. Because phosphorylation positively regulates AKT kinase activity, these results predict that the activity of genes downstream of AKT will be modulated in responsive cells exposed to lapatinib. In addition, AKT1 mRNA expression decreases 7- to 10-fold in BT474 and SKBr3 cells exposed to 1.0 μmol/L of lapatinib for 12 h (1 μmol/L was chosen as a clinically relevant concentration; ref. 33). In contrast, AKT1 mRNA decreases <2-fold in nonresponsive cells exposed to high doses of lapatinib (Fig. 1C).

It is well established that AKT kinases influence a number of important pathways in normal and tumor cells including cell proliferation, survival, and glucose metabolism (34, 35). The antiapoptotic effect of AKT is at least in part due to its role as a negative regulator of FOXO3A (36). Thus, the effect of lapatinib on FOXO3A RNA expression and phosphorylation was measured in BT474, SKBr3, MDA468, and T47D cells. BT474 and SKBr3 phosphoprotein analysis shows that AKT-mediated phosphorylation of FOXO3A was differentially down-regulated by lapatinib in the responsive cells (Fig. 2A). In addition, microarray data showed that FOXO3A RNA expression was differentially up-regulated by lapatinib in responsive cell lines (Fig. 2B). Furthermore, both the transcriptional and posttranscriptional effects of lapatinib on FOXO3A depend on the dose and length of the exposure (Fig. 2A and B). The latter observation suggests that the quantitative changes in *FOXO3A* transcription and the loss of FOXO3A phosphorylation are specific effects of lapatinib. These data also predict that FOXO3A function should be different in lapatinib-treated BT474 and SKBr3 cells as compared with MDA468 and T47D. This prediction was tested by measuring the expression of the FOXO3A target gene, *CDKN1B*, which codes for cell cycle inhibitor protein p27 (Fig. 2C and D). Immunoblot analysis shows that p27 protein increases in a lapatinib dose- and time-dependent manner in responsive cell lines BT474 and SKBr3 but not in nonresponsive cell lines (Fig. 2C). Microarray data shows that a large increase in p27 transcription occurs in BT474 and SKBr3 cells exposed to 0.1 or 1.0 μmol/L of lapatinib (Fig. 2D). Further studies showed that the proapoptotic FOXO3A target genes *TRAIL*, *HBP1*, and *BN1P3L* were also differentially induced by lapatinib in responsive breast cancer cells (data not shown). FOXO3A promotes cell cycle arrest by inhibiting the expression of cyclins D1 and D2 (37). In our study, lapatinib caused a strong dose- and time-dependent decrease in *CCND1* expression (the gene coding cyclin D1) in responsive cell lines but a moderate decrease in expression in nonresponsive cells (Table 2). Expression of CCND1 protein, cyclin D1 follows a similar pattern (data not shown). These data support the conclusion that *FOXO3A* and its downstream target genes are differentially induced in lapatinib-responsive breast cancer cells.

Previous studies suggest possible cross-talk between estrogen and progesterone-signaling pathways and the EGFR/ErbB2 signaling pathways (19, 20, 21). In addition, ER and PR status is considered a strong predictor for breast cancer prognosis (38), and ER-negative and PR-negative

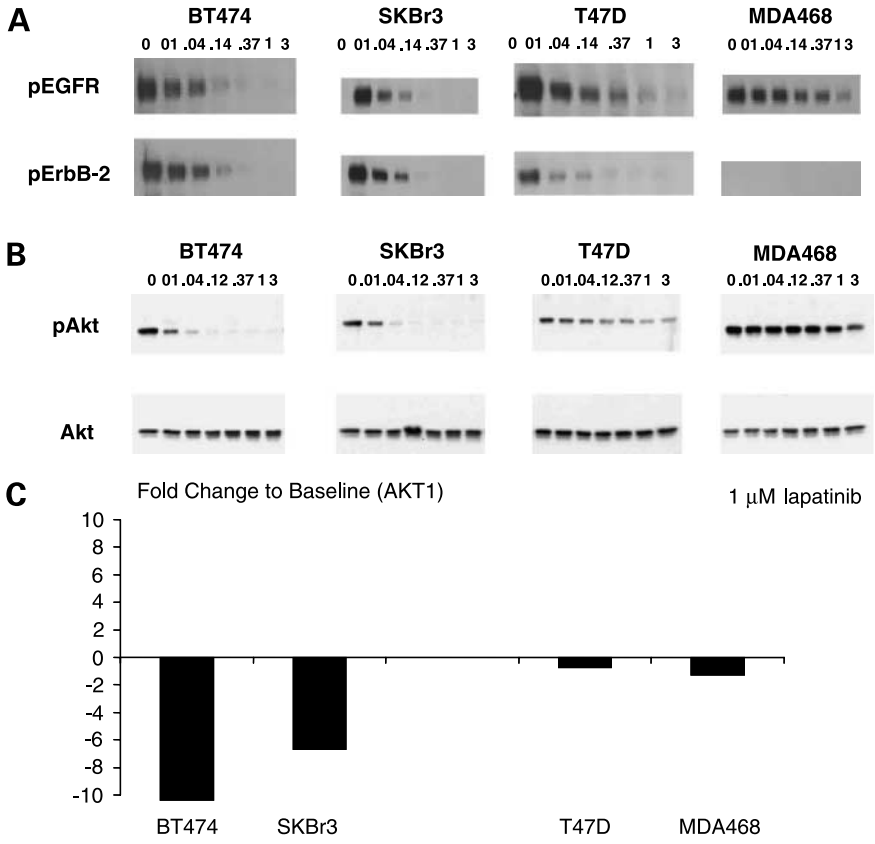

Figure 1. Phosphoprotein analyses of EGFR and ErbB2, and total AKT and microarray analyses of AKT1 mRNA in the presence and absence of lapatinib. **A,** expression of pEGFR and pErbB2 were detected by Western blot analysis using ECL. Lysates were prepared from cells treated with increasing doses of lapatinib for 6 h. **B,** total phospho-Akt (*pAkt*) and Akt expression were detected by Western blot analysis using ECL. Lysates were prepared from cells treated with increasing doses of lapatinib for 6 h. **C,** expression of AKT1 on a 12-h lapatinib (1 μmol/L) treatment in BT474, SKBr3, T47D, and MDA468 cells. A pair-wise fold change of AKT1 expression upon treatment with lapatinib compared with baseline untreated cells at 12 h (*Y-axis*).

breast tumors are consistently associated with poor breast cancer prognosis. The possibility that ER and/or PR signaling might play a role in the response to lapatinib was explored by measuring basal and induced transcription of the genes for ER and PR, *ESR1*, and *PGR* in responsive and nonresponsive breast cancer cells. The results are shown in Fig. 3. Moderate basal transcription of *ESR1* and *PGR* was detected in BT474 and T47D cells, but transcription of *ESR1* and *PGR* was not above background in SKBr3 and MDA468 cells (Fig. 3A). Notably, transcription of *ESR1* and *PGR* was induced 7- to 11-fold by lapatinib in BT474 and T47D cells (Fig. 3B). In contrast, statistically significant increases in *ESR1* or *PGR* transcription were not observed in SKBr3 and MDA468 cells. Thus, lapatinib seems to have a strong stimulatory effect on *ESR1* and *PGR* in cells with moderate basal levels of expression of these genes. This result suggests that ER and/or PR signaling may be up-regulated in some lapatinib-treated breast cancer cells.

The data presented above indicate that lapatinib significantly modulates the expression of more than one gene in the AKT pathway. This observation led us to examine the protein-protein and protein-gene interactions in the AKT pathway in greater detail using the Ingenuity Pathways Knowledge Base and TransFac. The results of this analysis are shown in Fig. 4. In this diagram of the AKT pathway, positive-interacting proteins are connected by red arrows, negative interacting proteins are connected by green arrows, and protein-DNA binding interactions are indicated by black arrows. The expression of each of these genes was quantified by microarray in the four breast cancer cell lines in the presence or absence of lapatinib, and the lapatinib-induced fold change in the expression of these genes is summarized in Table 2. After exposure to 1.0 μmol/L of lapatinib for 12 h, AKT1, MAPK9, HSPCA, IRAK1, and CCND1 RNAs are down-regulated by 7- to 22-fold in responsive breast BT474 and SKBr3 cells. In contrast, lapatinib-mediated down-regulation of these genes in the nonresponsive cells is moderate compared with the responsive cells. BAD, E2F3, TK1, and EIF2S1 RNAs were down-regulated ≈10-fold in either BT474 or SKBr3 cells, but the effect was not as strong in both nonresponsive cell lines. E2F1 and GRB2 RNAs were down-regulated to a similar extent by lapatinib in responsive and nonresponsive cell lines. As noted above, FOXO3A RNA was differentially up-regulated by lapatinib in responsive breast cancer cell lines (25- and 7-fold in BT474 and SKBr3 cells versus 4- and 3-fold in MDA468 and T47D cells, respectively). In summary, lapatinib strongly modulates the expression of proapoptotic genes in the AKT pathway in responsive but not in nonresponsive breast cancer cell lines.

Gene expression profiling also revealed the differential expression of cell cycle control genes in lapatinib-responsive breast cancer cells. In particular, CDC6, MCM2, and CDK4 RNAs are more strongly down-regulated in lapatinib-responsive than in nonresponsive cells (Fig. 5). CDK4

forms a complex with cyclin D1 (39), hence, it may be significant that both of these genes are strongly down-regulated in cells that respond to lapatinib. The transcription factor *E2F1* and genes that are directly regulated by it such as *RRM2*, *MCM2*, *MCM3*, *MCM7*, and *CDC45L* are down-regulated by lapatinib in responsive cell lines (Fig. 5; ref. 40). In addition, genes involved in DNA repair and DNA replication are also differentially expressed by lapatinib treatment specifically in responsive cells. These included genes such as *RAD51C* and inositol phosphate phosphatase-like 1 (*INPPL1*). In addition to being involved in DNA repair, *INPPL1*, which codes for SHIP2, is also associated with the AKT/mTOR signaling pathway (41).

Lapatinib treatment also differentially down-regulated key genes in glycolysis (phosphoglycerate kinase), the TCA pathway (ATP citrate lyase), and lipid and fatty acid metabolism [fatty acid synthase (FASN)] in responsive cells (Fig. 5). Key genes associated with glycolysis such as enolase 1, pyruvate kinase, and phosphoglycerate kinase were down-regulated by lapatinib in both responsive cell lines. The magnitude of decreased expression of these genes is much higher in BT474 cells compared with SKBr3 cells. For example, *PKM2* is 14-fold down-regulated in BT474 cells, whereas exhibiting a 5-fold decrease in SKBr3 cells. Baseline levels of *PKM2* expression are higher in BT474 cells compared with SKBR3 cells. However, on drug treatment, mRNA levels of *PKM2* in both cell lines are comparable (data not shown). This may contribute to the higher magnitude of change in BT474 cells compared with the SKBR3 cells. *FASN* is also differentially modulated in responsive cells. *FASN* is transcriptionally regulated by phosphatidylinositol-3-kinase and inhibits apoptosis in prostate cancer cells (42). Pharmacologic inhibition of FASN in breast cancers is reported to suppress HER2/Neu-mediated malignancies (43). The mechanism and significance of these gene expression changes are not yet known.

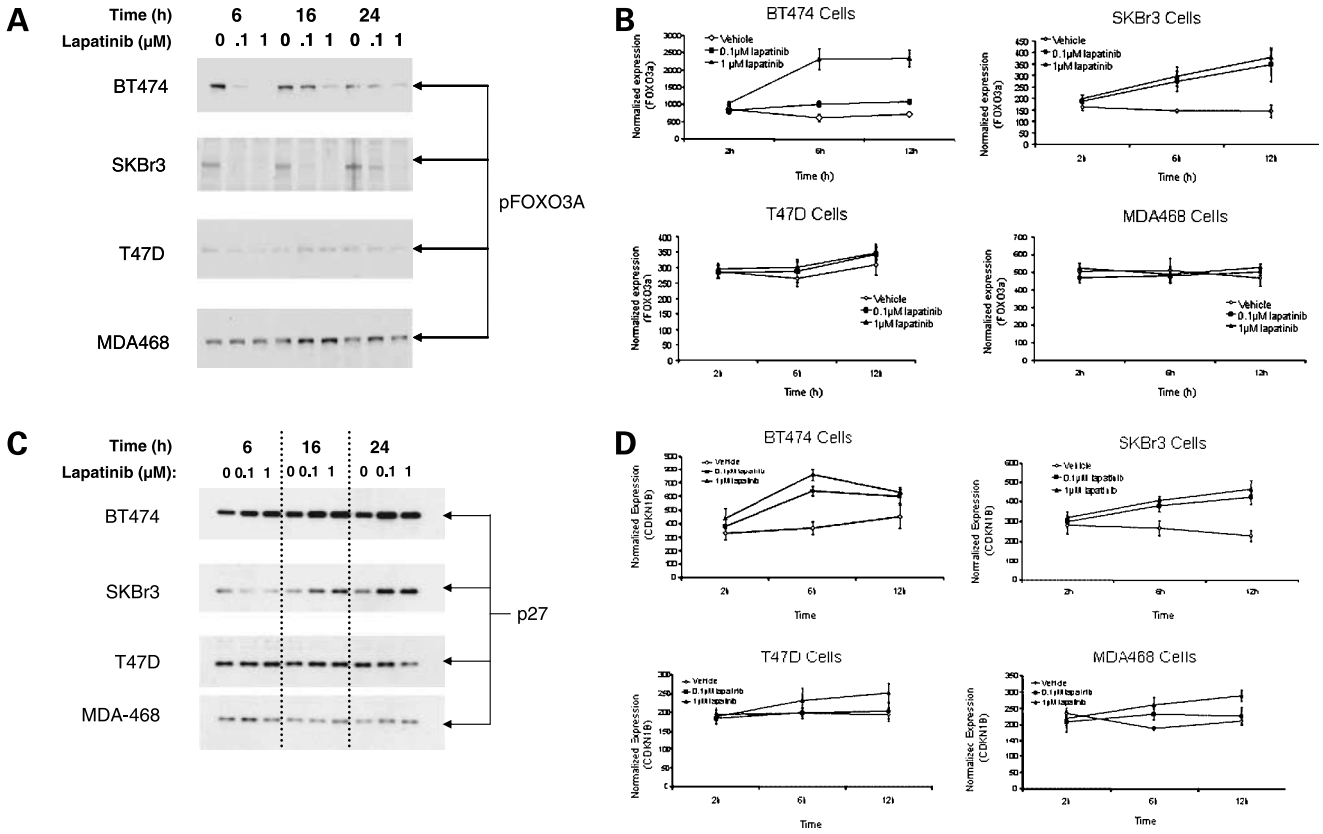

Figure 2. Microarray and phosphoprotein analysis of FOXO3A and its target protein p27. **A,** phospho-FKHRL1/FOXO3A protein was detected by Western blot analysis using ECL (BT474, MDA-468, and T47D cell lines) or IR Image Analysis (SKBr3 cells). Cells were treated with 0.1 or 1 μmol/L of lapatinib for 6, 16, or 24 h. **B,** kinetics and dose-dependence of the induction of FKHRL1/FOXO3A mRNA by lapatinib. Microarray analysis was done on BT474, SKBr3, T47D, and MDA468 cells treated with 0.1 or 1 μmol/L of lapatinib for 2, 6, or 12 h. Three independent replicates were prepared for each data point. Normalized intensities for the FKHRL1 (*FOXO3a*) probe set on the U133A chip. Control cells were treated with vehicle. **C,** p27 expression was detected by Western blot analysis using ECL. Cells were treated with 0.1 or 1 μmol/L of lapatinib for 6, 16, or 24 h. **D,** kinetics and dose-dependence of the induction of CDKN1B (p27) by lapatinib. Microarray analysis was done on BT474, SKBr3, T47D, and MDA468 cells treated with 0.1 or 1 μmol/L of lapatinib for 2, 6, or 12 h. Three independent replicates were prepared for each data point. Normalized intensities for the CDKN1B (p27) probe set on the U133A chip.

Table 2. Lapatinib-induced change in expression of genes in the ERB/AKT pathway at 12 h

Sequence ID	Name	T47D	MDA468	BT474	SKBR3
207163_s_at	AKT1	−0.8	−1.3	−10.4	−6.7
1861_at	BAD*	0.4	−0.1	−10.0	−2.4
203693_s_at	E2F3	−2.8	−4.1	−5.6	−11.3
2028_s_at	E2F1*	−4.4	−0.4	−4.1	−6.4
203218_at	MAPK9	−2.7	−6.8	−14.6	−11.8
215075_s_at	GRB2	−0.5	−2.5	−0.8	−3.9
211968_s_at	HSPCA*	−2.8	−4.8	−11.1	−7.5
204131_s_at	FOXO3A*	4.4	3.3	24.8	6.9
202338_at	TK1	−1.6	3.3	−9.6	−2.9
201587_s_at	IRAK1*	0.0	−4.7	−8.3	−22.1
201144_s_at	EIF2S1	−5.9	−5.0	−5.3	−9.8
208712_at	CCND1*	−7.33	−7.38	−17.1	−16.44

*Confirmation of array results for a subset of genes by quantitative real-time reverse transcription-PCR.

Discussion

Antitumor chemotherapy targeting receptor tyrosine kinases has variable efficacy in human breast cancers. To improve the understanding of the molecular basis of drug responsiveness in human breast tumors, this study compared phosphorylation changes and patterns of gene expression in breast cancer cell lines that are responsive or nonresponsive to the dual ErbB2/EGFR inhibitor lapatinib. The results suggest strong differential down-regulation of pAKT and AKT1 RNA and modulation of downstream genes in the AKT pathway in lapatinib-responsive cells as well as altered expression of steroid hormone genes and genes involved in cell cycle control and energy and fat metabolism. These data provide insight into the mechanism of cytotoxicity in lapatinib-responsive cells and may be useful in developing tools for optimizing receptor-targeted chemotherapy for patients with breast cancer.

Microarray gene expression profiling and targeted pathway analysis were used to assess the effect of lapatinib on the AKT pathway in breast cancer cells. Several striking differences were observed in lapatinib-responsive and nonresponsive cell lines in addition to the changes in pAKT. AKT1 mRNA was down-regulated 10.4- or 6.7-fold in responsive cell lines BT474 and SKBr3, respectively; in contrast, *AKT1* expression did not change significantly in nonresponsive T47D and MDA468 cells. *BAD1* is another AKT pathway gene that is down-regulated significantly in BT474 and SKBr3 cells (10.0- and 2.4-fold, respectively) but not in T47D and MDA468 cells. Several other genes in the

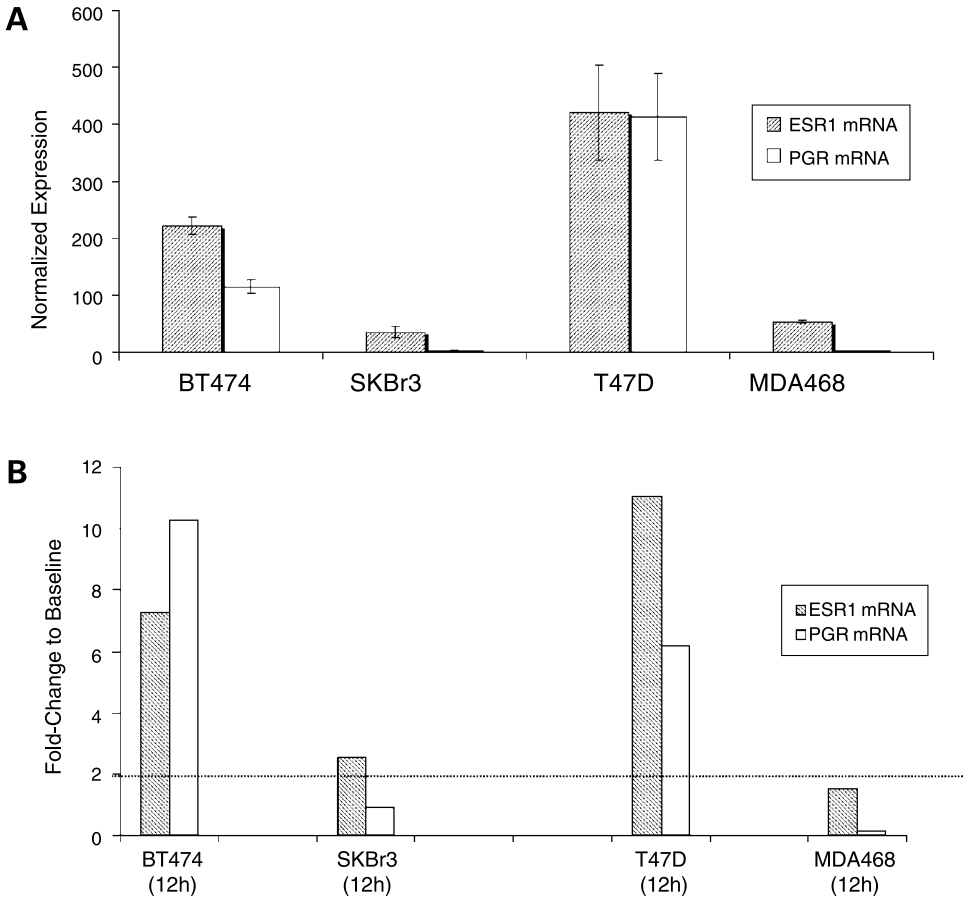

Figure 3. Basal and induced transcription of ESR1 and PGR. BT474, SKBr3, T47D, and MDA468 cells were treated in the presence or absence of lapatinib and cDNA was prepared for microarray analysis. **A,** basal expression of ESR1 and PGR was determined by microarray analysis of cDNA from the indicated cell lines grown in the absence of lapatinib for 12 h. Microarray Analysis Suite 5.0 – normalized intensities for ESR1 and PGR probe sets from the U133A chip. **B,** effect of lapatinib treatment on expression of ESR1 and PGR. A pair-wise fold change analysis relative to untreated control cells at the 12-h time point for the 1 μmol/L dose of lapatinib (*Y-axis*). *Dotted line,* minimum fold change value that is statistically significant.

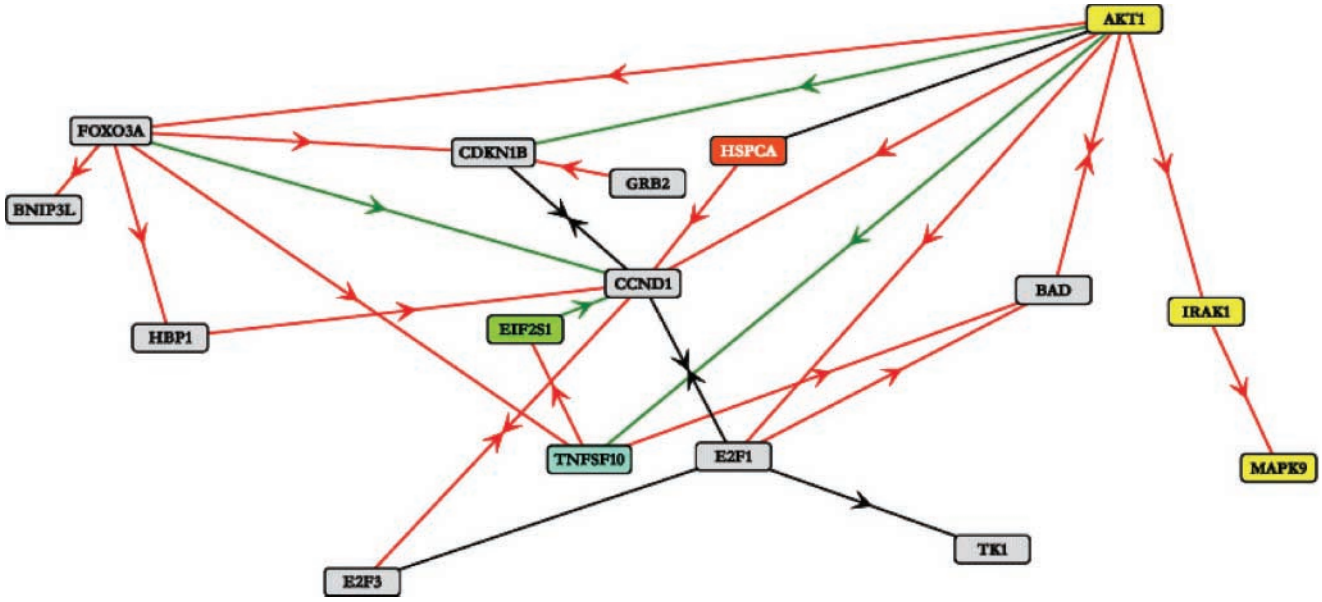

Figure 4. Connectivity network for the AKT signaling pathway. Protein-protein and protein-gene interactions involving AKT and genes downstream of AKT were identified using the Ingenuity Pathways Knowledge base and TransFac. Positive-interacting proteins (*red arrows*), negative-interacting proteins (*green arrows*), and protein-DNA binding interactions (*black arrows*).

AKT pathway (i.e., *E2F3*, *MAPK9*, *HSPCA*, *TK1*, *IRAK1*, and *CCND1*) were down-regulated in all four cell lines examined here, but the average magnitude of the change was much greater in responsive than in nonresponsive cells. Lastly, FOXO3A is up-regulated in responsive cell lines; this result was expected, because AKT negatively regulates the expression of *FOXO3A*. It is noteworthy that pFOXO3A is decreased and FOXO3A RNA is very strongly up-regulated in BT474 and SKBr3 cells (24.8- and 6.9-fold, respectively), whereas pFOXO3A and FOXO3A RNA changes are less pronounced in T47D and MDA468 cells. Thus, the cumulative effect of these gene expression changes and the decreases in pFOXO3A, although difficult to quantify, were expected to be very strong and far greater in BT474 and SKBr3 than in T47D and MDA468 cells.

Previous studies have shown that lapatinib is cytotoxic or cytostatic, depending on the tumor cell lines, inducing cell death or cell cycle arrest in sensitive cell lines (9). Results presented here provide suggestive evidence that lapatinib-induced cell death may be promoted by a FOXO3A-dependent mechanism that can be suppressed by active AKT. This conclusion is based on the fact that *FOXO3A* and FOXO3A target genes are differentially up-regulated, whereas AKT is differentially down-regulated in lapatinib-responsive breast cancer cells. The effect on *FOXO3A* expression is particularly large (25-fold) in BT474 cells. FOXO3A target genes including *CDKN1B*, *TRAIL*, *HBP1*, and *BN1P3L* are also significantly induced in lapatinib-responsive cells. Because the FOXO3A subpathway seems to be up-regulated by lapatinib and because FOXO3A is well-characterized as a positive inducer of apoptotic cell death, these data suggest that lapatinib-induced cytotoxicity may require FOXO3A. Additional experiments will be required to test this hypothesis directly, such as lapatinib challenge of isogenic FOXO3A-proficient and FOXO3A-deficient cell lines. Further testing is also required to determine if non–breast human tumor cells also show FOXO3A-dependent apoptosis in response to lapatinib.

FOXO3A may play another important role in lapatinib-responsive cells because previous studies indicate cross-talk between FOXO3A and ER signaling in breast cancer cells. Guo and Sonenshein (44) recently showed that FOXO3A binds to and stimulates expression from the *ESR1* promoter. The results presented here are consistent with the Guo and Sonenshein report because lapatinib induces *ESR1* and *PGR* expression in BT474 (7- and 11-fold) and T47D (10- and 6-fold) cells. However, BT474 cells are responsive to lapatinib and express a high level of FOXO3A in the presence of lapatinib, whereas T47D cells are not responsive to lapatinib and express a moderate level of FOXO3A in the presence of lapatinib. Thus, the exact mechanism by which lapatinib induces *ESR1* in BT474 and T47D cells is not clear at present. The up-regulation of *PGR1* in these two cell lines was expected because *PGR1* is induced by ER (45). These data also suggest that lapatinib-stimulated induction of *ESR1* and *PGR1* was not the apoptotic trigger per se in ER-positive breast cancer cells. Furthermore, because SKBr3 and MDA468 cells do not express ESR1 or PGR RNAs at a statistically significant level in the presence or absence of lapatinib, it is not possible to draw conclusions about the dependence on ER or PR status and response to lapatinib. MDA468 are known to have methylation of the CpG island of the ER gene as the mechanism for lack of ER expression (45), and therefore, ER expression would not be expected to

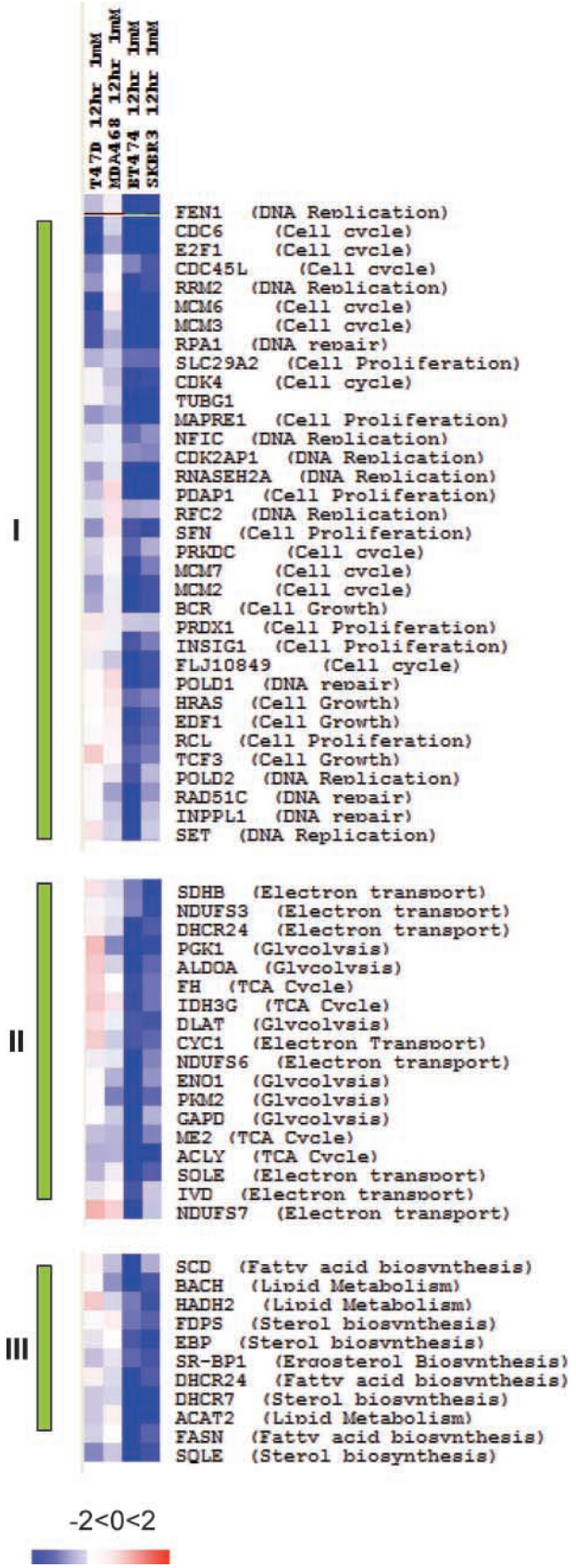

change upon lapatinib treatment. Further experiments are required to more completely understand the interaction between ER/PR and AKT1/FOXO3A signaling pathways in breast cancer cells. Additional influence of ER/PR expression in these cells may come from the modulation of the extracellular signal-regulated kinase/mitogen-activated protein kinase pathway which has also been linked to ER expression (46). Nevertheless, the present data suggests that lapatinib could act synergistically with an antiestrogenic compound to limit the growth of some breast tumor cells. Clinical trials combining lapatinib and letrozole are currently under way.

In addition to changes observed in the AKT signaling pathway, lapatinib treatment also results in differential expression of genes associated with cell cycle regulation. These genes are mostly involved with either G_1-S phase transition such as *CDC6*, *CDK4*, and the transcription factor *E2F1*, or in the prereplication complex machinery such as the *MCM2*, *MCM3*, *MCM6*, and *MCM7*. MCM expression peaks at the G_1-S boundary and this expression is regulated by E2F1 (40). Thus, lapatinib seems to modulate the expression of genes primarily associated with the G_1-S phase of the cell cycle.

Preliminary studies shown here also suggest that lapatinib might limit the growth of responsive cells by modulating the expression of critical factors in glycolysis, e.g., glyceraldehyde-3-phosphate dehydrogenase, enolase 1, and pyruvate kinase. Carcinogenesis and metastasis are intimately linked with increased glycolysis, and AKT-mediated resistance to growth factor withdrawal is associated with maintenance of glycolytic rate (47). Thus, it is not surprising that treatment with lapatinib results in the suppression of genes associated with glycolysis. Lapatinib treatment seems to deprive cells of energy not only via down-regulation of glycolysis but also by modulating genes in energy and fatty acid metabolism. FASN, an enzyme that is required for carbohydrate to fatty acid conversion, is highly expressed in breast cancers (48). Moreover, one mechanism of FASN-mediated tumorigenic activity may be via expression, activation, and cellular localization of HER2 (43). Our results show that lapatinib treatment results in the down-regulation of *FASN* as well as other genes in fatty acid biosynthesis and sterol biosynthesis such as the δ-9-desaturase, *SCD*, and 7-dehydrocholesterol reductase to a greater extent in responsive cell lines versus nonresponsive cell lines. Although further studies are needed to understand the significance of these gene expression changes, they could further limit growth in cells in which the AKT pathway has been down-regulated.

Figure 5. Cluster analysis of genes differentially expressed by lapatinib. The concentration of lapatinib was 1 μmol/L for all cell lines. Treatment groups were listed horizontally, whereas genes are listed vertically. Each cell represents a fold change of drug treated over control untreated cells at 12 h. *Red,* genes that were induced by lapatinib 2-fold or higher; *blue,* genes that are down-regulated by lapatinib by 2-fold or lower. *Cluster I,* genes involved in cell cycle control; *clusters II* and *III,* genes involved in energy utilization, glycolysis, and fatty acid metabolism.

In conclusion, this study shows that the efficacy of lapatinib in breast cancer cells correlates with its ability to down-regulate the AKT pathway and up-regulate the FOXO3A subpathway. Genes involved in cell cycle control, glycolysis, and fatty acid metabolism are also differentially affected. In addition, lapatinib induces *ESR1* and *PGR* expression in some breast cancer cell lines, and this may influence the outcome of combination therapy using lapatinib and antiestrogenic compounds. Additional studies are needed to determine if lapatinib acts in a similar manner in non–breast human cancer cells.

Acknowledgments

The authors thank Miriam Sander of Page One Editorial Services for her editorial assistance in writing this manuscript, Jennifer Hagen for technical assistance, and Matthew Newman and Shawn O'Brien for their help in uploading the microarray data into MIAME.

References

1. Yarden Y, Sliwkowski MX. Untangling the ErbB signaling network. Nat Rev Mol Cell Biol 2001;2:127 – 37.

2. Citri A, Skaria KB, Yarden Y. The deaf and the dumb: the biology of ErbB-2 and ErbB-3. Exp Cell Res 2003;284:54 – 65.

3. Schlessinger J. Ligand-induced, receptor-mediated dimerization and activation of EGF receptor. Cell 2002;110:669 – 72.

4. Olayioye MA. Update on HER-2 as a target for cancer therapy: intracellular signaling pathways of ErbB2/HER-2 and family members. Breast Cancer Res 2001;3:385 – 9.

5. Jorissen RN, Walker F, Pouliot N, Garrett TPJ, Ward CW, Burgess AW. Epidermal growth factor receptor: mechanisms of activation and signalling. Exp Cell Res 2003;284:31 – 53.

6. Baselga J, Arteaga CL. Critical update and emerging trends in epidermal growth factor receptor targeting in cancer. J Clin Oncol 2005;23: 2445 – 59.

7. Slamon DJ. The future of ErbB-1 and ErbB-2 pathway inhibition in breast cancer: targeting multiple receptors. Oncologist 2004;9:1 – 3.

8. Reid A, Vidal L, Shaw H, de Bono J. Dual inhibition of ErbB1 (EGFR/HER1) and ErbB2 (HER2/neu). Eur J Cancer 2007;43:481 – 9.

9. Rusnak DW, Lackey K, Affleck K, et al. The effects of the novel, reversible epidermal growth factor receptor/ErbB-2 tyrosine kinase inhibitor, GW2016, on the growth of human normal and tumor-derived cell lines *in vitro* and *in vivo*. Mol Cancer Ther 2001;2:85 – 94.

10. Wood ER, Truesdale AT, McDonald OB, et al. A unique structure for epidermal growth factor receptor bound to GW572016 (Lapatinib): relationships among protein confirmation, inhibitor off-rate, and receptor activity in tumor cells. Cancer Res 2004;64:6652 – 9.

11. Geyer CE, Forster J, Lindquist, D, et al. Lapatinib plus capecitabine for HER2-positive advanced breast cancer. N Engl J Med 2006;355: 2733 – 43.

12. Comis RL. The current situation: Erlotinib (Tarceva®) and Gefitinib (Iressa®) in non_small cell lung cancer. Oncologist 2005;10:467 – 70.

13. Slamon DJ, Clark GM, Wong SG, Levin WJ, Ullrich A, McGuire WL. Human breast cancer: correlation of relapse and survival with amplification of the HER-2-neu oncogene. Science 1987;235:177 – 82.

14. Lewis S, Locker A, Todd JH, et al. Expression of epidermal growth factor receptor in breast carcinoma. J Clin Pathol 1990;43:385 – 9.

15. Witton CJ, Reeves JR, Going JJ, Cooke TG, Bartlett JM. Expression of the HER1 – 4 family of receptor tyrosine kinases in breast cancer. J Pathol 2003;200:290 – 7.

16. Zeillinger R, Kury F, Czerwenka K, et al. HER-2 amplification, steroid receptors, and epidermal growth factor receptor in primary breast cancer. Oncogene 1989;4:109 – 14.

17. Konecny G, Pauletti G, Pegram M, et al. Quantitative association between HER-2/neu and steroid hormone receptors in hormone receptor-positive primary breast cancer. J Natl Cancer Inst 2003;95: 142 – 53.

18. Yamauchi H, Stearns V, Hayes DF. When is a tumor marker ready for prime time? A case study of c-erbB-2 as a predictive factor in breast cancer. J Clin Oncol 2001;19:2334 – 56.

19. Nicholson RI, McClelland RA, Robertson JF, Gee JM. Involvement of steroid hormone and growth factor crosstalk in endocrine response in breast cancer. Endocr Relat Cancer 1999;6:373 – 87.

20. Gutierrez MC, Detre S, Johnston S, et al. Molecular changes in tamoxifen-resistant breast cancer: relationship between estrogen receptor, HER-2, and p38 mitogen-activated protein kinase. J Clin Oncol 2005; 23:2469 – 76.

21. Schiff R, Massarweh SA, Shou J, Bharwani L, Mohsin SK, Osborne CK. Cross-talk between estrogen receptor and growth factor pathways as a molecular target for overcoming endocrine resistance. Clin Can Res 2004;10:331 – 6S.

22. Osborne CK, Shou J, Massarweh S, Schiff R. Crosstalk between estrogen receptor and growth factor receptor pathways as a cause for endocrine therapy resistance in breast cancer. Clin Can Res 2005;11: 865 – 70S.

23. Nicholson RI, Staka C, Boyns F, Hutcheson IR, Gee JMW. Growth factor-driven mechanisms associated with resistance to estrogen deprivation in breast cancer: new opportunities for therapy. Endocr Relat Cancer 2004;11:623 – 41.

24. Nicholson RI, Hutcheson IR, Britton D, et al. Growth factor signaling networks in breast cancer and resistance to endocrine agents: new therapeutic strategies. J Steroid Biochem Mol Biol 2005;93:257 – 62.

25. Chu I, Blackwell K, Chen S, Slingerland J. The dual EGFR/ErbB2 inhibitor, Lapatinib (GW572016), cooperates with tamoxifen to inhibit both cell proliferation- and oestrogen-dependent gene expression in antiestrogen-resistant breast cancer. Cancer Res 2005;65:18 – 25.

26. Chu Q, Goldstein L, Murray N, et al. A phase I, open-label study of the safety, tolerability and pharmacokinetics of Lapatinib (GW572016) in combination with letrozole in cancer patients. Proc Am Soc Clin Oncol 2005;23:3001.

27. Carter MC, Cockerill GS, Guntrip SB, Lackey KE, Smith KJ. Bicyclic heteroaromatic compounds [quinazolinamines and analogs] useful as protein tyrosine kinase inhibitors. PCT Int Appl, WO9935146, Glaxo Wellcome 1999.

28. Mager ME. Data analysis in biochemistry and biophysics. 1st ed. New York: Academic Press, Inc.; 1972.

29. Hardwicke JS, Yang Y, Zhang C, et al. Identification of biomarkers for tumor endothelial cell proliferation through gene expression profiling. Mol Cancer Ther 2005;4:413 – 25.

30. Rajagopalan D, Agarwal P. Inferring pathways from gene lists using a literature-derived network of biological relationships. Bioinformatics 2005; 21:788 – 93.

31. Rusnak DW, Alligood KJ, Hudson-Curtis B, et al. Assessment of epidermal growth factor receptor (EGFR, ErbB1) and ErbB2 protein expression levels and sensitivity to GW572016 in an expanded panel of human normal and transformed cell lines. Keystone Symposium, Protein kinases in cancer: the promise of molecular-based therapies, February 24 – 29, 2004, Tahoe City, CA, 305, p56.

32. Xia W, Mullin RJ, Keith BR, et al. Anti-tumor activity of GW572016: a dual tyrosine kinase inhibitor blocks EGF activation of EGFR/erbB2 and downstream Erk1/2 and AKT pathways. Oncogene 2002;21: 6255 – 63.

33. Burris HA III, Hurwitz HI, Dees EC, et al. Phase I safety, pharmacokinetics, and clinical activity study of lapatinib (GW572016), a reversible dual inhibitor of epidermal growth factor receptor tyrosine kinases, in heavily pretreated patients with metastatic carcinomas. J Clin Oncol 2005;23:5305 – 13.

34. Bellacosa A, Testa JR, Moore R, Larue L. A portrait of AKT kinases: human cancer and animal models depict a family with strong individualities. Cancer Biol Ther 2004;3:268 – 75.

35. Bellacosa A, Kumar CC, Di Cristofano A, Testa JR. Activation of AKT kinases in cancer: implications for therapeutic targeting. Adv Cancer Res 2005;94:29 – 86.

36. Kops GJ, Medema RH, Glassford J, et al. Control of cell cycle exit and entry by protein kinase B-regulated forkhead transcription factors. Mol Cell Biol 2002;22:2025 – 36.

37. Schmidt M, Fernandez de Mattos S, Van der Horst A, et al. Cell cycle inhibition by FoxO forkhead transcription factors involves downregulation of cyclin D. Mol Cell Biol 2002;22:7842 – 52.

38. Osborne CK. Steroid hormone receptors in breast cancer management. Breast Cancer Res Treat 1998;51:227 – 38.

39. Serrano M, Hannon GJ, Beach D. A new regulatory motif in cell-cycle control causing specific inhibition of cyclin D/CDK4. Nature 1993;6456: 704 – 7.

40. Ohtani K, Iwanaga R, Nakamura M, et al. Cell growth-regulated expression of mammalian MCM5 and MCM6 genes mediated by the transcription factor E2F. Oncogene 1999;18:2299 – 309.

41. Aman JM, Lamkin TD, Okada H, Kurosaki T, Ravichandran KS. The inositol phosphatase SHIP inhibits Akt/PKB activation in B cells. J Biol Chem 1998;273:33922 – 8.

42. Van de Sande T, De Schrijver E, Heyns W, Verhoeven G, Swinnen JV. Role of the phosphatidylinositol 3′-kinase/PTEN/Akt kinase pathway in the overexpression of fatty acid synthase in LNCaP prostate cancer cells. Cancer Res 2002;62:642 – 6.

43. Menendez JA, Mehmi I, Verma VA, Teng PK, Lupu R. Pharmacological inhibition of fatty acid synthase (FAS): a novel therapeutic approach for breast cancer chemoprevention through its ability to suppress Her-2/neu (erbB-2) oncogene-induced malignant transformation. Mol Carcinog 2004;41:164 – 78.

44. Guo S, Sonenshein GE. Forkhead box transcription factor FOXO3a regulates estrogen receptor α expression and is repressed by the Her-2/neu/phosphatidylinositol 3-kinase/Akt signaling pathway. Mol Cell Biol 2004;24:8681 – 90.

45. Lapidus RG, Nass SJ, Davidson NE. The loss of estrogen and progesterone receptor gene expression in human breast cancer. J Mammary Gland Biol Neoplasia 1998;3:85 – 94.

46. Oh AS, Lorant LA, Holloway JN, Miller DL, Kern FG, El-Ashry D. Hyperactivation of MAPK induces loss of ERα expression in breast cancer cells. Mol Endocrinol 2001;15:1344 – 59.

47. Plas DR, Talapatra S, Edinger AL, Rathmell JC, Thompson CB. Akt and Bcl-xL promote growth factor-independent survival through distinct effects on mitochondrial physiology. J Biol Chem 2001;276:12041 – 8.

48. Wang Y, Kuhajda FP, Li JN, et al. Fatty acid synthase (FAS) expression in human breast cancer cell culture supernatants and in breast cancer patients. Cancer Lett 2001;167:99 – 104.